ISSN 1615-9306 · JSSCCJ 44 (3) 2021 · Vol. 44 · No. 3 · February 2021

Journal of SEPARATION SCIENCE

3|2021

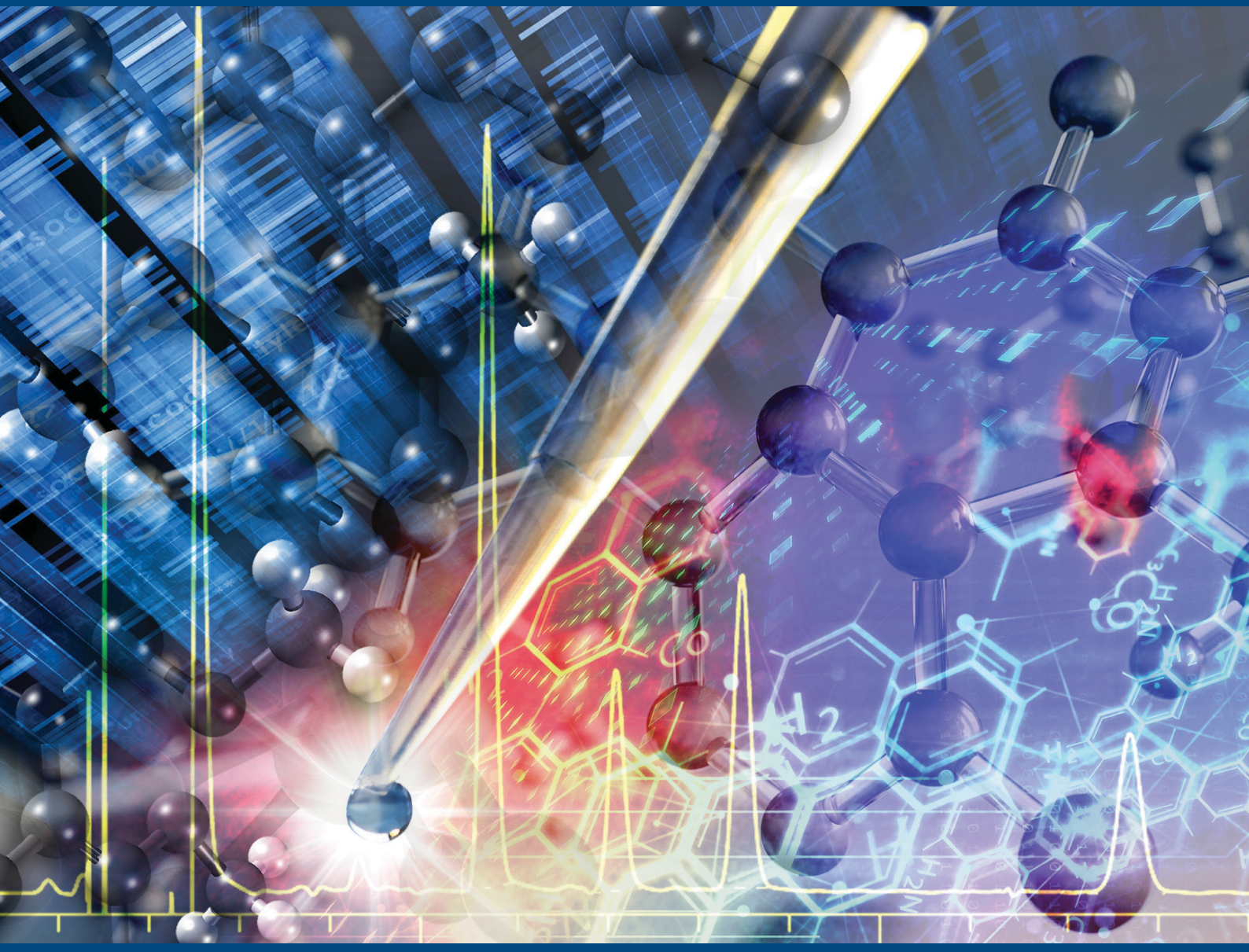

Methods
Chromatography · Electroseparation

Applications
Biomedicine · Foods · Environment

www.jss-journal.com

WILEY-VCH

Received: 13 August 2020 | Revised: 16 November 2020 | Accepted: 17 November 2020

DOI: 10.1002/jssc.202000883

JOURNAL OF SEPARATION SCIENCE

RESEARCH ARTICLE

Comparison of separation modes for microchip electrophoresis of proteins

Thushara N. Samarasinghe | **Yong Zeng**[#] | **Carey K. Johnson**

Department of Chemistry, University of Kansas, Lawrence, Kansas, USA

Correspondence
Carey K. Johnson, Department of Chemistry, University of Kansas, 1140 Gray-Little Hall, Lawrence, KS 66045,
Email: ckjohnson@ku.edu

[#]Current Address: Department of Chemistry, University of Florida, Gainesville, Florida, USA

Separation of a set of model proteins was tested on a microchip electrophoresis analytical platform capable of sample injection by two different electrokinetic mechanisms. A range of separation modes—microchip capillary zone electrophoresis, microchip micellar electrokinetic chromatography, and nanoparticle-based sieving—was tested on glass and polydimethylsiloxane/glass microchips and with silica-nanoparticle colloidal arrays. The model proteins calmodulin (18 kiloDalton), bovine serum albumin (66 kDa), and concanavalin (106 kDa) were labeled with Alexa Fluor 647 for laser-induced fluorescence detection. The best separation and resolution were obtained in a silica-nanoparticle colloidal array chip.

KEYWORDS
capillary electrophoresis, electrokinetic injection, laser induced fluorescence detection, microchip electrophoresis

1 | INTRODUCTION

Despite the introduction of novel techniques, protein separation with microfluidic devices is still challenging due to the unique characteristics of proteins [1–6]. Among the most significant challenges encountered in microchip separations of proteins are the similarity in electrophoretic mobilities for different proteins, protein adsorption to surfaces, Joule heating, and the need for sensitive detection. Recent advances include the application of methods such as capillary gel electrophoresis and micellar electrokinetic chromatography (reviewed in [2,4,5]), the development of coatings to improve performance (reviewed in [2,3]), and use of polymeric materials [7].

Here we study the effectiveness of several separation methods by microchip electrophoresis (MCE) with a set of model proteins. MCE-based protein separation methods are generally adapted from the conditions optimized for conventional CE [8,9]. CE uses high voltages and exhibits relatively short separation times with small sample volumes to attain high separation efficiencies of up to millions of theoretical plates [10]. Microchip electrophoresis coupled with sensitive detection methods has been utilized to further improve electrophoretic protein separations [11,12].

The aim of this work was to compare three MCE separation modes: microchip capillary zone electrophoresis (MCZE), MEKC, and silica-nanoparticle based sieving, coupled with different chip substrates, glass, polydimethylsiloxane (PDMS)/glass, and silica-nanoparticle colloidal array chips, for separation of a set of proteins spanning a large range in molecular mass. A further goal was to contrast separations in the presence of EOF with separations where EOF is suppressed. Calmodulin (CaM), BSA, and concanavalin A (ConA) were selected as model proteins for this study.

Abbreviations: AF647, Alexa Fluor 647; CaM, calmodulin; ConA, concanavalin A; DDM, *n*-dodecyl-β-D-maltopyranoside; HEPES, 4-(2-hydroxyethyl)−1-piperazineethanesulfonic acid; HPMC, hydroxypropyl methylcellulose; MCE, microchip electrophoresis; MCZE, microchip zone electrophoresis; PDMS, polydimethylsiloxane; TBE, tris-borate EDTA

2 | MATERIALS AND METHODS

2.1 | Materials and reagents

T34C-CaM was expressed in *E. coli* and purified according to a previously published method [13]. The Cys residue in T34C-CaM was labeled with Alexa Fluor 647 (AF647) maleimide (Molecular Probes, Eugene OR) following methods previously described [14]. Commercially available BSA and concanavalin A (ConA) conjugated with AF647 were purchased from Molecular Probes (Eugene, OR).

SU-8 10 negative photoresist and silicon wafers were purchased from Micro-Chem (Newton, MA) and Silicon (Boise, ID), respectively. Polydimethylsiloxane (PDMS) and a curing agent were purchased from Ellsworth Adhesives (Minneapolis, MN). Silica nanobeads were purchased from Bangs Laboratories (Fishers, IN). Fused silica capillaries (id 50 μm and od 364 μm) were purchased from Polymicro Technology (Molex, Lisle, IL). *n*-Dodecyl-β-D-maltopyranoside (DDM), 4-(2-hydroxyethyl)−1-piperazineethanesulfonic acid (HEPES), and sodium hydroxide were purchased from Fisher Scientific (Fair Lawn, NJ). Platinum (Pt) wire was purchased from Ted Pella (Redding, CA). Hydoxypropyl methylcelulose (HPMC), tris-borate EDTA (TBE) 10× buffer (CE grade), boric acid, and SDS were acquired from Sigma–Aldrich (St. Louis. MO). All reagents and samples were prepared with doubly-deionized water from an ultrapure water system (Barnstead, Dubuque, IA). Samples, reagents, and run buffers were filtered by 0.22-μm syringe filter before separations.

PDMS-based microchips were fabricated by standard soft lithography at the Adams Micro-Fabrication facility (University of Kansas, KS). To develop a raised structure (mold) for electrophoresis channels, SU-8 negative photoresist was spin-coated on a 4-inch silicon wafer up to a thickness of ∼16 μm with a spin coater (Brewer Science, Rolla, MO). The wafer was soft baked on a programmable hot plate (Thermo Scientific, Ashville, NC) at 65°C for 2 min, followed by 95°C for 5 min. AutoCad LT 2004 (Autodesk, San Rafael, CA) was used to create microfluidic channel designs, which were printed onto a transparency film at a resolution of 50,000 dpi (Infinite Graphics, Minneapolis, MN). The transparency film was aligned on top of the photoresist coated wafer and exposed to UV light (ABM, San Jose, CA). After the exposure, the wafer was baked at 65°C for 2 min followed by 95°C for 10 min. SU-8 developer was used to develop the channel structures, and the wafer was washed with isopropyl alcohol and dried with nitrogen gas. Finally, the developed wafer was "hard-baked" at 175°C for 2 h. The depth of the PDMS microfluidic channels, was measured with a surface profiler (Alfa Step-200, Tencor Instruments, Mountain View, CA). PDMS microfluidic channels were cast using a 10:1 mixture of the elastomer and the curing agent, respectively. The channels were ∼40 μm wide and ∼16 μm deep.

Glass microchips were fabricated by the Adams Micro-Fabrication facility (University of Kansas), as described previously [15,16]. Silica-nanoparticle chips were constructed as described previously [12]. Briefly, a chip with simple "T" format (10 mm separation channel and 4 mm side arms) was fabricated from an approximately 5-mm thick PDMS layer and cured at 60°C overnight. Reservoirs were made with a 2-mm biopsy puncher. PDMS chips were sealed to clean glass slides. Monodisperse plain silica beads 170 nm and 400 nm in diameter (10% m/v, Bangs Laboratories, Fishers, IN) were introduced by controlled evaporation of water from the buffer waste reservoir (see Supporting Information Figure S2) [12], allowing colloidal arrays to assemble as 3D structures inside the microchannels [17,18]. The growth of the array was stopped by replacing the colloidal suspension in the reservoirs with water.

2.2 | Methods

Microfluidic channels were checked under a microscope, and any particles were removed with 0.1 M NaOH or isopropyl alcohol with pressure. PDMS/glass and glass chips were conditioned with 0.1 M NaOH and purified water for 5 min each, followed by run buffer (which was specific to the experiment) for another 5 min. Before the separation, the device was checked again for any clogging. Similarly, after self-assembly of the colloidal array, silica-nanoparticle microfluidic devices were equilibrated with the run buffer for 20 min.

Microchips were mounted on an X–Y translational stage (Newport, Irvine, CA) situated on a Nikon TE 300 microscope. A 633-nm He-Ne laser beam was passed through a neutral density filter wheel (Newport, Irvine, CA) to adjust the beam power. The laser beam power was measured by an optical power meter (Pro-lite Technology, Bedfordshire, UK). The laser beam was reflected by a dichroic mirror (ZT640rdc, Chroma, Bellows Falls, VT) through the microscope objective (LUCPLFLN Plan 40×, 0.4 NA, 2.5-mm working distance, Olympus Corp., Center Valley, Pa) and into the microchannel. Fluorescence emission was collected by the objective, reflected through the C-port of the microscope through a band-pass filter (Q660LP, Chroma, Bellows Falls, VT), and detected by an avalanche photodiode photon counting module (SPCM AQR-14, PerkinElmer, Waltham, MA). A high voltage was applied between the reservoirs of the microfluidic device by a power supply with four independently-controlled high-voltage channels

(HV-RACK-4-250, UltraVolt, Ronkonkoma, NY). Voltage was delivered to microchip reservoirs via Pt leads.

Protein samples were denatured at 95°C in the presence of 3.5 mM SDS for 5 min prior to separations. For gated injections in the separation state, high voltages were applied to the reservoir sample and buffer reservoirs such that the sample and the run buffer fluid flow established a gated cross section at the intersection of the vertical and horizontal channels. For a desired injection time (for example 0.3 s), the potential of the buffer reservoir was switched to zero so that a sample plug flowed through the cross junction due to cathodic electro-osmotic flow (EOF). The potential of the buffer reservoir was reestablished, and the sample plug was allowed to pass along the separation channel. (A schematic representation of the reservoir voltages is shown in the Supporting Information Figure S3.) Pinched injections with pull-back were used for separations with suppressed EOF. For injection, a high positive voltage was applied to the buffer-waste reservoir and low positive voltages to the sample and sample waste reservoirs, such that negatively charged sample species moved towards the buffer waste reservoir with "pull-back" in the sample channel to prevent sample leakage into the separation channel after injection. (Voltages for pinched injection are depicted schematically in Figure S4.)

CE was performed in a bare fused silica capillary placed in a Beckman P/ACE MDQ instrument (Beckman, Fullerton, CA). Samples were dissolved in a background electrolyte (BGE) containing 3.5 mM SDS. Laser-induced fluorescence was excited at 635 nm and collected through a band-pass filter, 705 nm, bandpass 72 nm (ET705/72 Chroma, Bellows Falls, VT). Capillaries were conditioned with methanol and 1 M NaOH for 20 min prior to use, followed by 5 min with water at 7×10^4 Pa pressure. Separations were carried out at 20°C. Samples were injected into the capillary by pressure injections (3×10^3 Pa for 10 s). After each run, the capillary was washed with methanol, 1 M HCl, 1 M NaOH, and water for 2 min each, followed by the BGE (75 mM boric acid adjusted to pH 9.2 with NaOH, and 3.5 mM SDS) for 3 min before injection of the sample.

3 | RESULTS

The molecular masses of the three model proteins increase in the order CaM (~18 kDa) < BSA (~66 kDa) < ConA (~106 kDa) (molecular masses include attached Alexa Flour 647). Molecular masses, *pI* values, and hydropathicity values for the three proteins are listed in Supporting Information, Table S1. After denaturation by heat in the presence of SDS (3.5 mM), protein analytes are expected to have a uniform negative charge density and a spherical shape.

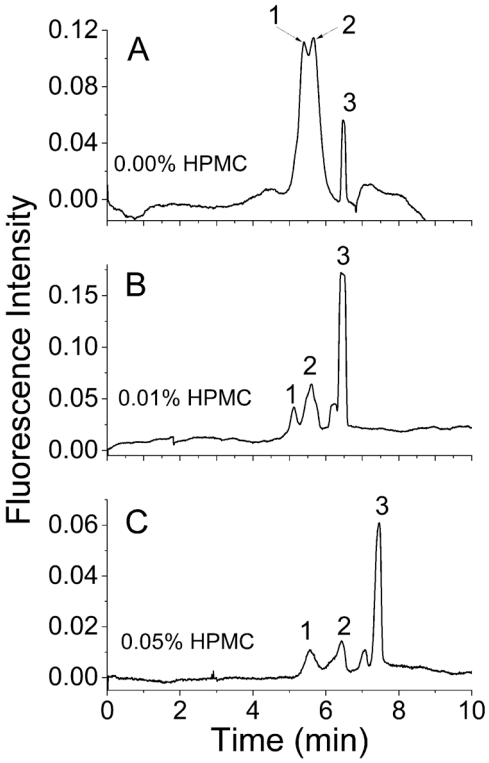

FIGURE 1 **Separation of three model proteins with a bare silica capillary.** Capillary length: 0.3-m, length to detector: 0.21 m, id: 50 μm, BGE: 75 mM boric acid adjusted to pH 9.2 with NaOH and 3.5 mM SDS, (**A)** No HPMC added to the run buffer. The applied field strength was 1.94×10^4 V/m. Peaks 1, 2, and 3 were identified as ConA, BSA, and CaM, respectively. The concentrations of CaM, BSA, and ConA were ~40, ~40, and ~20 nM, respectively. (**B)** The same separation conditions but with 0.01% (m/v) HPMC added to the run buffer. The concentrations of CaM, BSA, and ConA were ~40, ~20, and ~10 nM, respectively. (**C)** The same separation conditions but with 0.05% (m/v) HPMC added to the run buffer. The concentrations of CaM, BSA, and ConA were ~20, ~10, and ~5 nM, respectively

3.1 | Capillary electrophoresis separation of model proteins

Conventional CE was carried out as a benchmark for the separation of the model proteins. The separation of SDS-protein complexes with bare silica capillaries is depicted in Figure 1. The migration order was ConA, BSA, and CaM. In the absence of HPMC (Figure 1A) ConA and BSA were not fully resolved. With successive runs resolution decreased, migration times changed, and band broadening was observed (data not shown). This suggests that the adsorption of the proteins onto the capillary wall contributed to the relatively high and noisy background and partially resolved peaks. Similar effects have been reported previously for bare capillaries [19].

Adsorption of proteins to the capillary wall can degrade separations and affect the stability of electro-osmotic flow [20]. Therefore, HPMC was added to the buffer to coat

the capillary walls. Separations with 0.01 and 0.05 % (m/v) HPMC are shown in Figure 1B and C. With the addition of 0.01% (m/v) HPMC (Figure 1B), the three analytes were separated with improved resolution and repeatability. A slight increase of migration times of analytes in the presence of HPMC can be attributed to the reduced EOF caused by the addition of HPMC [21,22]. Upon increasing the HPMC concentration to 0.05% (m/v) the separation improved further (Figure 1C). Separation parameters of the model proteins for conventional CE are given in the Supporting Information (Table S2).

3.2 | Separation of model proteins by microchip electrophoresis

Glass microchips were used for microchip electrophoresis due to their high stability at high voltages compared to PDMS substrates. Furthermore, large reservoirs can be cast in glass chips to increase the buffer and sample volume and hence to minimize the effects of Joule heating and buffer evaporation. Separations of the model proteins were also attempted in PDMS/glass chips under a variety of buffer and separation conditions. However, good separations were not achieved (data not shown).

Figure 2 shows the separation of the model proteins with glass chips. Figure 2A shows results with gated injection into a 0.10-m separation channel on a serpentine glass chip with a BGE consisting of boric acid adjusted to pH 9.2 with sodium hydroxide and 3.5 mM SDS for separation of the model proteins by MCZE. The three model proteins migrated in under 100 s and were detected in the order of ConA < CaM < BSA. The observed migration order does not follow a consistent trend with respect to the molecular masses of the three proteins. Interactions with the glass surface may retard the migration of BSA, since the BGE did not contain any surface modifiers other than SDS that might have restricted adsorption of proteins. Repeatability in four consecutive runs is shown in the Supporting Information Figure S5. In separations without SDS, severe changes in migration times, peak heights, and peak shapes were observed in repeated separations (data not shown).

Figure 2B shows results obtained with an organic detergent, DDM (a water-soluble, non-ionic disaccharide derivative with a C_{10} linear hydrocarbon chain) as a dynamic coating agent [23]. DDM reduces EOF and helps to minimize surface adsorption proteins [23,24]. The buffer recipe (20 mM HEPES, 0.1% (m/v) DDM, 3.5 mM SDS, with pH adjusted to 7.5 with NaOH) used in this separation was initially reported by Zare and co-workers for a 3-cm long PDMS chip [23]. The separation conditions offered good repeatability (Supporting Information Figure S6) without changes in migration times and peak shapes. This suggests

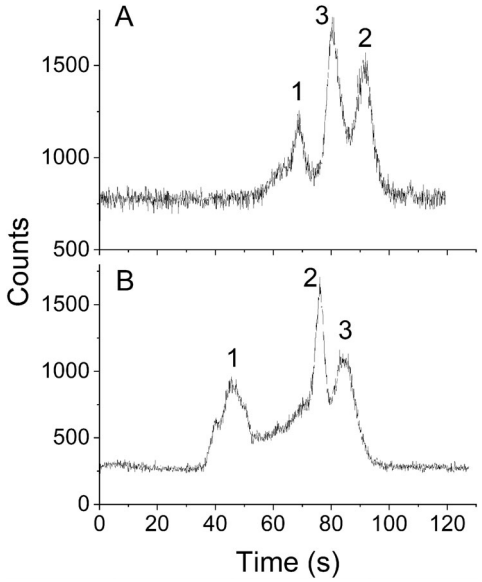

FIGURE 2 **Separation of the model proteins on glass chips.** Peak 1, 2, and peaks 3 were identified as ConA, BSA, and CaM, respectively. **(A)** MCZE on a serpentine glass chip. The separation conditions were as follows: BGE 50 mM boric acid adjusted to pH 9.2 with NaOH and 3.5 mM SDS, separation potential 7.5 kV, field strength ~7.50×10^4 V/m, injection time 0.3 s, and length to detector ~0.09 m. **(B)** MEKC on a 0.05-m glass chip. BGE: 20 mM HEPES, pH 7.5, 0.1% (m/v) DDM, and 3.5 mM SDS. Separation voltage and length to detector were 2500 V and ~0.04 m, respectively. The separation field strength was 5.00×10^4 V/m. Gated injection time was 0.5 s. A: Peak 1, peak 2, peak 3 are ConA, BSA, and CaM, respectively

reduced protein adsorption onto the channel walls in the presence of DDM. Further, the low conductivity HEPES buffer at lower pH likely created a lower EOF [23] than the high pH boric acid buffer used for MCZE (Figure 2A). The observed migration order was ConA < BSA < CaM (Figure 2B). Hence the result of addition of DDM and change in buffer conditions was a change in migration order but without substantial improvement in the separation.

3.3 | Separation of protein standards by microfluidic devices with silica-nanoparticle colloidal arrays

Silica colloidal crystal arrays afford an alternative separation mechanism in microdevices [1,12]. The colloidal array was formed in the separation channel of a PDMS chip with a glass base [1,12,25,26]. PDMS/glass chips were cast with wide channels (~100 μm) from a mold with a thick PDMS layer (~5 mm), resulting in relatively deep reservoirs. This accommodates adequate volumes (~20 μL) in reservoirs and hence decreases the drying effect of the colloidal array. Low electric fields ($4.0\text{-}6.0 \times 10^3$ V/m) were used to decrease Joule heating. Sample plugs were introduced by pinched injection.

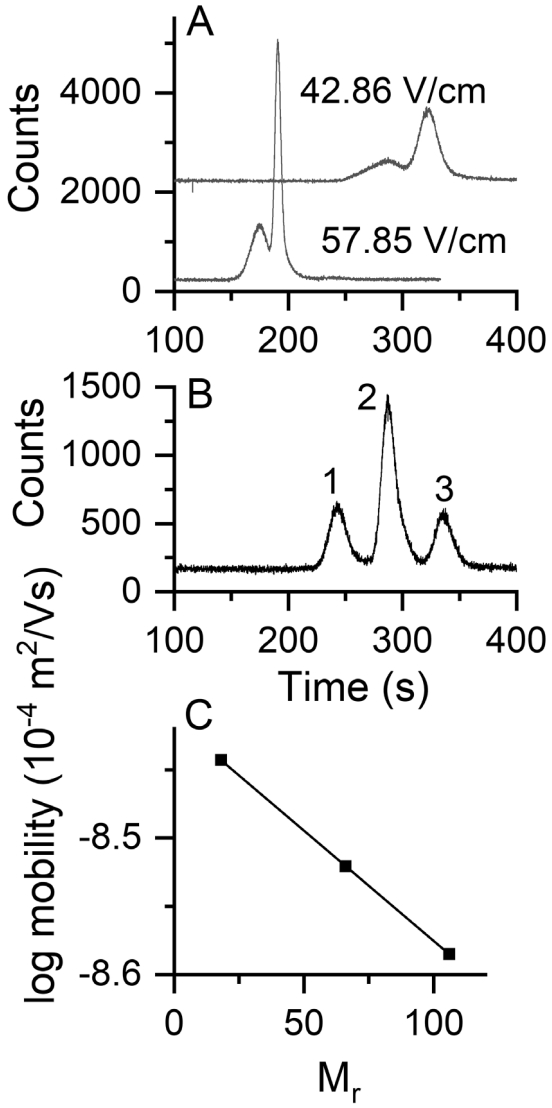

FIGURE 3 **Separation of protein standards by silica-nanoparticle colloid array microfluidic devices.** The buffer was 4X TBE, pH 8.5, 3.5 mM SDS. The buffer and sample channels were ~5-mm long, and the separation channel was 10-mm long. The diameter of the reservoirs was 1.5 mm. **(A)** separation of a mixture of three protein standards with a 400 nm array with field strengths 4.3×10^3 V/m and 5.8×10^3 V/m (the former plotted with an offset of 2000 counts). **(B)** Separation with a 170 nm array. The separation field strength was 5.8×10^3 V/m. Peaks 1, 2, and 3 were identified as CaM, BSA, and ConA, respectively. **(C)** Semilog plot of the apparent mobilities of SDS-protein complexes vs protein molecular masses with a least-squares linear fit ($n = 7$). Fit parameters are $\log \mu = -0.0016\, M_r - 8.4$ with $R^2 = 0.9999$, where M_r is the relative molecular mass. The error bars show the standard error

Figure 3A shows the separation of the three model proteins with a colloidal array of 400-nm beads. A BGE with high ionic strength (4× TBE, pH 8.3, consisting of 360 mM tris-borate, 8.0 mM EDTA) was used to reduce EOF [12,27]. High resistance to fluid flow in the sieving media also reduced the effect of EOF. Electropherograms were obtained with two different field strengths. Two different colloidal arrays (particle size 170 and 400 nm) were used to separate SDS-protein complexes. Different sizes of nanoparticles create different pore sizes for size-based separation of biomolecules [12]. The standard proteins were partially resolved with 400-nm beads, which offer a pore size of ~60 nm [12,26]. Separation was greatly improved with a 170 nm silica-nanoparticle array (pore size, ~26 nm) despite the short separation distance of ~5 mm (Figure 3B).

Figure 3C shows a plot of the log apparent mobility versus molecular mass. The apparent mobility, μ_{app} of a protein was calculated by

$$\mu_{app} = \frac{L_d/t_m}{V/L_t} \quad (1)$$

where L_d is the length to the detector and L_t is the length of the separation channel, t_m is the migration time, and V is the separation voltage. The peak-to-peak resolution of CaM and BSA ($R_{1,2}$), and BSA and ConA ($R_{2,3}$) were 2.9 and 2.6, respectively. The calculated average peak capacity and the number of theoretical plates for the silica-nanoparticle colloidal array were 14 and 1.5×10^5 m^{-1}, respectively. The average separation efficiency of the silica-nanoparticle colloidal array, the height equivalent to one theoretical plate, was 6.5×10^{-6} m. Accordingly, of the separation methods surveyed, the silica-nanoparticle colloidal array provided the best separation of the model proteins.

4 | DISCUSSION

Macromolecules such as proteins exhibit low mobility under electric fields, but relatively high nonspecific adsorption [21,22,28–32], including interactions with the capillary or microchannel walls. CE separations are significantly impaired by transient or permanent adsorption of proteins onto capillary walls [20]. BSA, for example, shows both hydrophilic and hydrophobic interactions with a glass surfaces at physiological pH [32,33]. Indeed, BSA has been used to coat negatively-charged glass and polymeric substrates to minimize nonspecific adsorption of other proteins [31]. Even though the surface is negatively charged, anionic proteins may adsorb onto the channel wall by electrostatic and hydrophobic interactions [21,28–30]. This results in a non-uniform ζ-potential over the length of the capillary [24], and consequently a zonal variation of the EOF, resulting in turn in band broadening, asymmetric peaks, poor separation efficiency, and poor reproducibility of migration times [24,34–36]. One approach to mitigate these effects, is to suppress interactions with the capillary surface with charged or uncharged coatings.

Dynamic coating and modification of run buffers are the two most common methods used for surface

TABLE 1 Migration order for separation methods

Method	Migration order	Mechanism
Capillary zone electrophoresis	ConA < BSA < CaM	Electrophoretic mobility relative to EOF
Microchip zone electrophoresis	ConA < CaM < BSA	Electrophoretic mobility relative to EOF
Glass chip with surface modifier (DDM)	ConA < BSA < CaM	Possible MEKC
Colloidal array	CaM < BSA < ConA	Sieving

modification in both CE and MCE [8,11,37,38]. SDS was included in all BGEs and sample reagents as a dynamic coating agent. Interaction of SDS molecules in the run buffer with the microchannel or capillary wall [39] is thought to reduce adsorption of proteins onto the microchannel or capillary wall without changing the EOF [39,40]. Permanent or dynamic coating of the capillary walls can be achieved with water-soluble small molecules or nonionic and ionic polymers [24]. In the present case, the detergent DDM and the polymer-like cellulose derivative HPMC were used as buffer coating agents [21,23]. Other methods are focused on improving performance through variation of pH, ionic strength, organic additives, and surfactants [21,24,41]. Without SDS, peak heights and peak shapes changed significantly in consecutive runs, band broadening increased, and sensitivity decreased (data not shown). We conclude that the presence of SDS in the BGE is very important for achieving reproducible and efficient separations.

Table 1 summarizes the migration order observed for the methods tested in this study. CZE without HPMC showed poor separation (Figure 1A), but with a migration order consistent with higher electrophoretic mobility (in the direction opposite of the EOF) for the protein with lowest molecular mass. Poor separation is consistent with previous reports that there is little difference in the electrophoretic mobilities of SDS-protein complexes in open capillaries [40,42–44]. Separation improved in the presence of HPMC (Figure 1B and C), with migration in order of decreasing size.

Migration in reverse order of size was not observed by MCZE in a glass microchip, with CaM migrating faster than BSA (Figure 2A). Reduction of the EOF with DDM in addition to SDS resulted in migration in the reverse order of molecular mass (Figure 2B). Addition of DDM reduces the critical micelle concentration (CMC) of SDS to 0.26 mM [23] with the formation of mixed micelles. The concentration of SDS in this experiment was ten-fold higher than the CMC. Interaction of the proteins with DDM-SDS micelles affects the separation, suggesting possible separation by MEKC. The partitioning of large molecules such as proteins inside micelles is unlikely, and thus the exact separation mechanism of large molecules under MEKC is unclear [22]. The extent of interaction of micelles with a protein is likely to depend on protein size and the number of hydrophobic residues. This suggests that separation occurred by MEKC with CaM partitioning most favorably with DDM-SDS micelles and ConA least favorably.

The masses of the three proteins are very different and hence size-based separations (capillary gel electrophoresis and nanoparticle colloidal array) were more successful than separations by CZE, which is based on the charge-to-size ratio, or micellar electrokinetic chromatography (MEKC), which is based on differential interactions of proteins with the micellar phase. We conclude that sieving is more likely to be effective for separation of a set of proteins with significantly different molecular masses.

Nonconventional methods such as nano-structured arrays open new possibilities. Zeng and Harrison introduced a sieving-based technique using self-assembled silica-nanoparticle colloidal arrays [12]. In this work, we used nanoparticle arrays to separate the model proteins. With the colloidal nanoparticle array, migration occurred in the order of increasing molecular mass, consistent with sieving. The apparent linear dependence of ln μ on molecular mass (Figure 3B) is consistent with free-volume (Ogston) sieving models [12,17,25,26,45–47]. The model assumes that the ratio of electrophoretic mobility, μ, to the mobility in free solution μ_0 is equal to the fraction f of the total volume in a porous medium that can be occupied by the analyte during migration, given by [46–48]:

$$\frac{\mu}{\mu_0} = f = e^{-KC} \tag{2}$$

where C is the density of sieving medium, K is the retardation factor with $K \propto R_g^2$ [49], and [45]

$$R_g = R_0 N^{1/2} \tag{3}$$

where R_0 is a constant for denatured proteins and N is the number of amino acids in the polypeptide chain. On average $N = M_r/110$, where M_r is the relative molecular mass of the protein. Considering the above parameters, the

mobility ratio is given by

$$\frac{\mu}{\mu_0} = e^{-aM_r} \quad (4)$$

where a is a collection of constants. Hence $\ln(\mu/\mu_0)$ is predicted to be linear with respect to the molecular mass M_r.

The linearity of the plot of $\ln \mu$ versus M_r suggests that $\ln \mu_0$ depends only weakly on the size of the analyte. A number of studies [42,43] have shown that the electrophoretic mobility of proteins can be modeled by an equation of the form

$$\mu_0 = A\frac{q}{M_r^p} + B \quad (5)$$

where q is the charge of the analyte, A and B are constants, and p has a value between 1/3 and 2/3, which indicates a much weaker dependence of $\ln \mu_0$ on M_r compared to $\ln \mu$. Furthermore, for proteins coated with SDS, q itself increases with M. Indeed, Takagi and co-workers found that the electrophoretic mobilities of proteins in the presence of SDS are essentially independent of molecular mass for proteins with M_r greater than ~15 000 [44], which includes all three proteins in this study, a result that is consistent with the poor separation we observed with CZE and MCZE.

5 | CONCLUDING REMARKS

The efficacy of several variants of microchip electrophoresis was tested for separation of three model proteins with detection by laser-induced fluorescence. Surface modification was essential to improve the resolution and separation efficiency. MCE with electrokinetic injection was demonstrated in a 0.10-m serpentine glass chip. Similarly, separation in the presence of DDM-SDS micelles was achievable in a 0.05-m glass chip. However, the best separation was obtained with a silica-nanoparticle chip, showing that sieving is effective at separation of the model proteins. To further optimize separation efficiency, we anticipate that two-dimensional separation, combining, for example, silica nanoparticle sieving with MCZE, would significantly enhance peak capacity and resolution.

ACKNOWLEDGMENTS

We thank Prof. Sue Lunte and Prof. Chris Culbertson for invaluable advice. We thank Wenju Xu and Yiqiu Yin for fabrication and assembly of the silica-nanoparticle chips. We thank Ryan Grigsby, Adams Micro Fabrication Facility, University of Kansas, for writing the LabVIEW programs, and Ken Ratzlaff, Instrumentation Design Laboratory, University of Kansas, for designing and building the high voltage relay box. This work was supported by a Patton Trust Research Development Grant from the Kansas City Area Life Sciences Institute.

CONFLICT OF INTEREST

The authors have declared no conflict of interest.

ORCID

Carey K. Johnson https://orcid.org/0000-0002-4207-8039

REFERENCES

1. Wirth MJ, Separation media for microchips. Anal Chem 2007;79:800–8.
2. Dawod M, Arvin NE, Kennedy RT, Recent advances in protein analysis by capillary and microchip electrophoresis. Analyst. 2017;142:1847–66.
3. Štěpánová S, Kašička V, Analysis of proteins and peptides by electromigration methods in microchips. J Sep Sci 2017;40:228–50.
4. Štěpánová S, Kašička V, Recent developments and applications of capillary and microchip electrophoresis in proteomics and peptidomics (2015–mid 2018). J Sep Sci 2019;42:398–414.
5. Štěpánová S, Kašička V, Recent applications of capillary electromigration methods to separation and analysis of proteins. Anal Chim Acta. 2016;933:23–42.
6. Ouimet CM, D'amico CI, Kennedy RT, Droplet sample introduction to microchip gel and zone electrophoresis for rapid analysis of protein-protein complexes and enzymatic reactions. Anal Bioanal Chem 2019;411:6155–63.
7. Barrios-Romero MDM, Crevillen AG, Diez-Masa JC, Development of an SDS-gel electrophoresis method on su-8 microchips for protein separation with lif detection: Application to the analysis of whey proteins. J Sep Sci 2013;36:2530–7.
8. Jorgenson JW, Lukacs KD, Capillary zone electrophoresis. Science. 1983;222:266–72.
9. Gordon MJ, Huang X, Pentoney SL Jr., Zare RN, Capillary electrophoresis. Science. 1988;242:224–8.
10. Hutterer KM, Jorgenson JW, Ultrahigh-voltage capillary zone electrophoresis. Anal Chem 1999;71:1293–7.
11. Tran NT, Ayed I, Pallandre A, Taverna M, Recent innovations in protein separation on microchips by electrophoretic methods: An update. Electrophoresis. 2010;31:147–73.
12. Zeng Y, Harrison DJ, Self-assembled colloidal arrays as three-dimensional nanofluidic sieves for separation of biomolecules on microchips. Anal Chem 2007;79:2289–95.
13. Devore MS, Gull SF, Johnson CK, Reconstruction of calmodulin single-molecule FRET states, dye-interactions, and CaMKII peptide binding by multinest and classic maximum entropy. Chem Phys 2013;422:238–45.
14. Price ES, Devore MS, Johnson CK, Detecting intramolecular dynamics and multiple Förster resonance energy transfer states by fluorescence correlation spectroscopy. J Phys Chem B. 2010;114:5895–902.
15. Scott DE, Grigsby RJ, Lunte SM, Microdialysis sampling coupled to microchip electrophoresis with integrated amperometric detection on an all-glass substrate. Chemphyschem. 2013;14:2288–94.

16. Allen PB, Chiu DT, Calcium-assisted glass-to-glass bonding for fabrication of glass microfluidic devices. Anal Chem 2008;80:7153–7.
17. King SB, Dorfman KD, Role of order during ogston sieving of DNA in colloidal crystals. Anal Chem 2013;85:7769–76.
18. Dorfman KD, King SB, Olson DW, Thomas JD, Tree DR, Beyond gel electrophoresis: Microfluidic separations, fluorescence burst analysis, and DNA stretching. Chem Rev 2013;113:2584–667.
19. Verzola B, Gelfi C, Righetti PG, Protein adsorption to the bare silica wall in capillary electrophoresis quantitative study on the chemical composition of the background electrolyte for minimising the phenomenon. J Chromatogr A. 2000;868:85–99.
20. Dolnik V, Capillary electrophoresis of proteins 2003–2005. Electrophoresis. 2006;27:126–41.
21. Doherty EA, Meagher RJ, Albarghouthi MN, Barron AE, Microchannel wall coatings for protein separations by capillary and chip electrophoresis. Electrophoresis. 2003;24:34–54.
22. Shadpour H, Soper SA, Two-dimensional electrophoretic separation of proteins using poly(methyl methacrylate) microchips. Anal Chem 2006;78:3519–27.
23. Huang B, Kim S, Wu H, Zare RN, Use of a mixture of n-dodecyl-beta-d-maltoside and sodium dodecyl sulfate in poly(dimethylsiloxane) microchips to suppress adhesion and promote separation of proteins. Anal Chem 2007;79:9145–9.
24. Gilges M, Kleemiss MH, Schomburg G, Capillary zone electrophoresis separation of basic and acidic protiens using poly(vinyl alcohol) coating in fused silica capillaries. Anal Chem 1994;66:2038–46.
25. Han J, Fu J, Schoch RB, Molecular sieving using nanofilters: Past, present and future. Lab Chip. 2008;8:23–33.
26. Birdsall RE, Koshel BM, Hua Y, Ratnayaka SN, Wirth MJ, Modeling of protein electrophoresis in silica colloidal crystals having brush layers of polyacrylamide. Electrophoresis. 2013;34:753–60.
27. Wu D, Regnier FE, Sodium dodecyl sulfate-capillary gel electrophoresis of proteins using non-cross-linked polyacrylamide. J Chromatogr A. 1992;608:349–56.
28. Dolnik V, Wall coating for capillary electrophoresis on microchips. Electrophoresis. 2004;25:3589–601.
29. Pallandre A, De Lambert B, Attia R, Jonas AM, Viovy JL, Surface treatment and characterization: Perspectives to electrophoresis and lab-on-chips. Electrophoresis. 2006;27:584–610.
30. Liu J, Lee ML, Permanent surface modification of polymeric capillary electrophoresis microchips for protein and peptide analysis. Electrophoresis. 2006;27:3533–46.
31. Shadpour H, Musyimi H, Chen J, Soper SA, Physiochemical properties of various polymer substrates and their effects on microchip electrophoresis performance. J Chromatogr A. 2006;1111:238–51.
32. Jeyachandran YL, Mielczarski E, Rai B, Mielczarski JA, Quantitative and qualitative evaluation of adsorption/desorption of bovine serum albumin on hydrophilic and hydrophobic surfaces. Langmuir. 2009;25:11614–20.
33. Larsericsdotter H, Oscarsson S, Buijs J, Structure, stability, and orientation of BSA adsorbed to silica. J Colloid Interf Sci 2005;289:26–35.
34. Towns JK, Regnier FE, Impact of polycation adsorption on efficiency and electroosmotically driven transport in capillary electrophoresis. Anal Chem 1992;64:2473–8.
35. Hjertén S, Kubo K, A new type of ph- and detergent-stable coating for elimination of electroendosmosis and adsorption in (capillary) electrophoresis. Electrophoresis. 1993;14:390–5.
36. Potoček B, Gaš B, Kenndler E, Štědrý M, Electroosmosis in capillary zone electrophoresis with non-uniform zeta potential. J Chromatogr A. 1995;709:51–62.
37. Manabe T, Capillary electrophoresis of proteins for proteomic studies. Electrophoresis. 1999;20:3116–21.
38. Hajba L, Guttman A, Recent advances in column coatings for capillary electrophoresis of proteins. TrAC-Trend Anal Chem 2017;90:38–44.
39. Nagata H, Tabuchi M, Hirano K, Baba Y, Microchip electrophoretic protein separation using electroosmotic flow induced by dynamic sodium dodecyl sulfate-coating of uncoated plastic chips. Electrophoresis. 2005;26:2247–53.
40. Gudiksen KL, Gitlin I, Whitesides GM, Differentiation of proteins based on characteristic patterns of association and denaturation in solutions of SDS. Proc Natl Acad Sci USA. 2006;103:7968–72.
41. Schomburg A, Kirchner H, Lopez-Hanninen E, Menzel T, Rudolph P, Korfer A, Fenner M, Poliwoda H, Atzpodien J, Hepatic and serologic toxicity of systemic interleukin-2 and/or interferon-alpha. Evidence of a risk-benefit advantage of subcutaneous therapy. Am J Clin Oncol 1994;17:199–209.
42. Rickard EC, Strohl MM, Nielsen RG, Correlation of electrophoretic mobilities from capillary electrophoresis with physicochemical properties of proteins and peptides. Anal Biochem 1991;197:197–207.
43. Compton BJ, Electrophoretic mobility modeling of proteins in free zone capillary electrophoresis and its application to monoclonal antibody microheterogeneity analysis. J Chromatogr A. 1991;559:357–66.
44. Karim MR, Shinagawa S, Takagi T, Electrophoretic mobilities of the complexes between sodium dodecyl sulfate and various peptides or proteins determined by free solution electrophoresis using coated capillaries. Electrophoresis. 1994;15:1141–6.
45. Viovy J-L, Electrophoresis of DNA and other polyelectrolytes: Physical mechanisms. Rev Mod Phys 2000;72:813–72.
46. Ogston AG, The spaces in a uniform random suspension of fibres. T Faraday Soc 1958;54:1754–7.
47. Rodbard D, Chrambach A, Unified theory for gel electrophoresis and gel filtration. Proc Natl Acad Sci USA. 1970;65:970–7.
48. Morris CJ, Morris P, Molecular-sieve chromatography and electrophoresis in polyacrylamide gels. Biochem J 1971;124:517–28.
49. Slater GW, Kenward M, Mccormick LC, Gauthier MG, The theory of DNA separation by capillary electrophoresis. Curr Opin Biotech 2003;14:58–64.

SUPPORTING INFORMATION

Additional supporting information may be found online in the Supporting Information section at the end of the article.

How to cite this article: Samarasinghe TN, Zeng Y, Johnson CK. Comparison of separation modes for microchip electrophoresis of proteins. *J Sep Sci*. 2021;44:744–751.
https://doi.org/10.1002/jssc.202000883